Available online at www.sciencedirect.com
ScienceDirect
Journal of Power Sources 170 (2007) 145–149
JOURNAL OF POWER SOURCES
www.elsevier.com/locate/jpowsour

Short communication

Plasma spray synthesis of ultra-fine YSZ powder

Zhenwei Wang [a,*], Rob Hui [a], Nikica Bogdanovic [b], Zhaolin Tang [b], Sing Yick [a], Yongsong Xie [a], Igor Yaroslavski [b], Alan Burgess [b], Radenka Maric [a], Dave Ghosh [a]

[a] *Institute for Fuel Cell Innovation, National Research Council Canada, 4250 Wesbrook Mall, Vancouver, BC V6T 1W5, Canada*
[b] *Northwest Mettech Corp., 467 Mountain Highway, North Vancouver, BC V7J 2L3, Canada*

Received 11 March 2007; received in revised form 30 March 2007; accepted 3 April 2007
Available online 18 April 2007

Abstract

A plasma spray process has been developed for the mass production of nanopowders for solid oxide fuel cells (SOFCs) and significant technical developments have been achieved during the past 2 years. Ultra-fine powders of 8 mol% yttria-stabilized zirconia (YSZ) were produced directly from a precursor solution via plasma spray process. The powders were characterized by X-ray diffraction (XRD), nitrogen absorption technique (BET), transmission electron microscopy (TEM), particle size analysis (PSA), and thermogravimetric analyses (TG). The as-sprayed YSZ powders with cubic phase were obtained without obvious impurity species. BET surface area of the sprayed powder reached as high as 27 $m^2\ g^{-1}$, indicating an equivalent particle size of 37 nm. The powder showed mostly spherical with mean size of about 100–200 nm by TEM results. Introduction of an organic additive resulted in a significantly increased specific surface area, accompanied by a slight decrease in grain size. This plasma spray process has the potential to be a less costly and time saving one for nanopowder production than the existing wet chemistry processes.

Keywords: Ultra-fine powder; YSZ; Plasma spray; Synthesis; Particle size

1. Introduction

Solid oxide fuel cells (SOFCs) are currently at the forefront of R&D into new generations of energy conversion systems, owing to their highly efficient and environmentally friendly nature. So far, SOFCs have not been commercialized due to technical obstacles, reliability problems and especially expensive costs. Oxygen ionic conductors of rare earth doped zirconia are widely adopted as electrolytes and electrode components in both anodes and cathodes to extend the triple-phase-boundaries (TPB) for better output performance [1,2]. Traditional methods for the production of zirconia-based electrolyte powder are based mostly on chemical co-precipitation, such as co-precipitation followed by azeotropically distilling in *n*-butanol [3]. The powder from precipitation shows broad particle size distribution and grain agglomeration and therefore needs more post-treatments. These shortages in turn result in poor sintering properties and electrochemical reactivity during SOFC operation. Many novel techniques have been developed oriented to highly homogeneous and ultra-fine powders in recent years, such as microwave synthesis [4], homogeneous precipitation [5], sol–gel processes [6–7], molecular decomposition processes [8], mechanical alloying [9], spray-pyrolysis [10–12], hydrothermal [13–16] and solvothermal [17] synthesis, and polymerization-combustion routes, etc. [18–23]. Significant advances have been achieved by these excellent studies. However, for the mass production of a commercial powder, the cost and yield of the process should also be taken into consideration. Plasma spraying (PS) technique offers a clean, controllable, and directional heat source. Reaction temperatures are much higher than that obtained by fossil fuels, so it can accelerate chemical reactions by several orders of magnitude. Reaction time is short and controllable and is much shorter than traditional wet-chemistry routes. PS processing is also a well-established and proven technology due to the low cost and simplicity of the process. It has been widely used in a variety of applications, such as thermal-barrier coatings (TBCs) [24], wear-resistance coatings [25] and the layer deposition for SOFCs [26–28]. So far, the effort to produce oxide powder for SOFC through plasma spray routine is still very limited [29–31]. In this study, an effort was made

* Corresponding author. Tel.: +1 604 221 5604; fax: +1 604 221 3001.
E-mail address: Zhenwei.Wang@nrc-cnrc.gc.ca (Z. Wang).

0378-7753/$ – see front matter © 2007 Elsevier B.V. All rights reserved.
doi:10.1016/j.jpowsour.2007.04.024

to develop a process for the production of ultra-fine powders. The powders of 8 mol% yttria-stabilized zirconia (YSZ) were produced and characterized.

2. Experimental

2.1. Plasma spray processing

Zirconium oxynitrate hydrate ($ZrO(NO_3)_2{\cdot}xH_2O$ solution) and yttrium nitrate hexahydrate ($Y(NO_3)_3{\cdot}6H_2O$ (both are from Blue Line Corp., USA) were first confirmed with the ZrO_2 solid contents by heat-treating the solution. Both chemicals were mixed with desired stoichiometry and ball-milled overnight into a well-dispersed precursor solution. The schematic diagram for the plasma spraying system is given in Fig. 1. The whole system can be divided into three subsystems: precursor solution delivery subsystem, plasma spray subsystem, and powder collection subsystem. The YSZ precursor solution was pumped into an internal nozzle by compressed air through a two-fluid atomizer. The atomized precursors were decomposed in the plasma stream to form the fine powders. The sprayed powders were then collected in a chamber with bag filters. The collection chamber was filled with de-ionized water to cool down the hot powder. When high flow rate and high organic additive content were applied under low plasma power in order to reduce the particle size of the powders, the as-sprayed powders were calcined at 600 °C for 2 h to burn off the leftover additives.

2.2. Powder characterization

X-ray diffraction technique (XRD) was used to identify the phase structure of the powders. XRD patterns were collected in a Bruker D8 Advance diffractometer using nickel-filtered Cu Kα radiation ($k = 0.1541$ nm). The XRD experiments were carried out in the 2θ range of 20–80° with 0.02° step^{-1} at a scan speed of 1° min^{-1}. The powder specific surface area was measured by nitrogen adsorption at 77 k using an automatic Beckman Coulter (SA3100 surface area analyzer). Before analysis, the samples were dried at 120 °C for 30 min in an oven to remove the absorbed moisture, then degassed in vacuum at 120 °C for 15 min. Based on the BET specific surface area (S) obtained, equivalent grain size D_{BET} is calculated according to the following equation:

$$D_{BET} = \frac{6}{(\rho \cdot S)}$$

In this equation, ρ is the theoretic density of the solid particles. For 8 mol% yttria-stabilized zirconia powder with pure cubic structure, ρ is 5.95 g cm^{-3}. Particle size distribution was analyzed using a Beckman Coulter (N4 plus submicron particle size analyzer). The powders were dispersed in de-ionized water with 1 wt.% DARVIN C as dispersant and strongly supersonicated for 5 min before particle size analysis was performed. The morphology and particle size were also investigated using a Hitachi H-1600 transmission electron microscope (TEM). Thermogravimetric analyses (TG) of the powder were carried out using a Hi-Res TGA 2950 thermogravimetric analyzer (TA Instruments) with temperature ramping rate of 10 °C min^{-1} up to 800 °C in air.

3. Results and discussion

3.1. Processing control

The properties of the sprayed YSZ powder can be affected by many parameters such as solution concentration, feeding rate, plasma power, composition of plasma gas, solvents and precursors, size of the atomization nozzle, air quenching or water quenching and post-treatment, etc. In order to optimize these spraying parameters, specific surface areas from nitrogen physical adoption (BET) were tested for each YSZ sample as an indicator. It is shown that about five times increase of specific surface area has been achieved during the past 2 years, as demonstrated in Fig. 2. The technical developments are gradually achieved both by the optimization of every subsystem of the plasma spray processing, i.e. precursor solution delivery subsystem, plasma spray subsystem, and powder collection

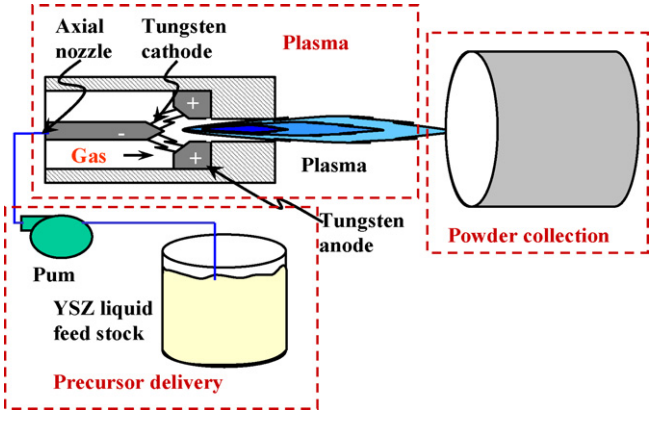

Fig. 1. Schematic diagram of the plasma spraying system for the production of ultra-fine powder.

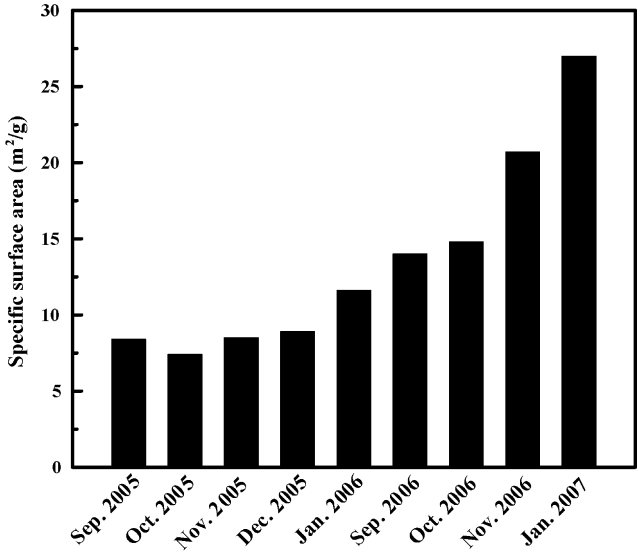

Fig. 2. Technical development during the past 2 years indicated by BET value.

subsystem and by the post-treatment of sprayed YSZ powder. It should be mentioned that so far, some parameters have not been systematically investigated.

3.2. Phase structure

Yttria doped zirconia has about seven different phases with yttria concentration ranging from zero to 15 mol%. Amongst these structures, 8 mol% yttria-stabilized zirconia with cubic phase shows the highest oxygen ionic conductivity and therefore is usually adopted as the solid electrolytes for solid oxide fuel cells. Fig. 3 gives the XRD pattern of the as-sprayed YSZ powder. The powder shows a pure cubic structure without any detectable impurity peak after spraying. It can also be found that the diffraction peaks are obviously widened, which suggested a reduced crystalline size.

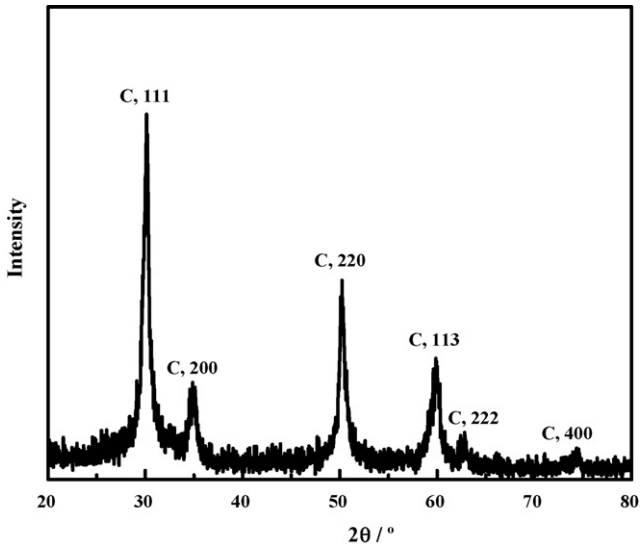

Fig. 3. XRD pattern of the plasma sprayed YSZ powder.

3.3. Particle size

Fig. 4 gives the TEM images of the sprayed powder with different magnification (Fig. 4A, 200k; B, 20k; C and D, 5k). The powder suspension for TEM observation of Fig. 4D is more concentrated than that of Fig. 4C. From Fig. 4A and B, the mean particle size can be estimated at about 100–200 nm. No extra large particles (>5 μm) can be found in TEM photos. Fig. 4C and D show more particle morphology with varying suspension content for TEM observation. Large particles can be found more

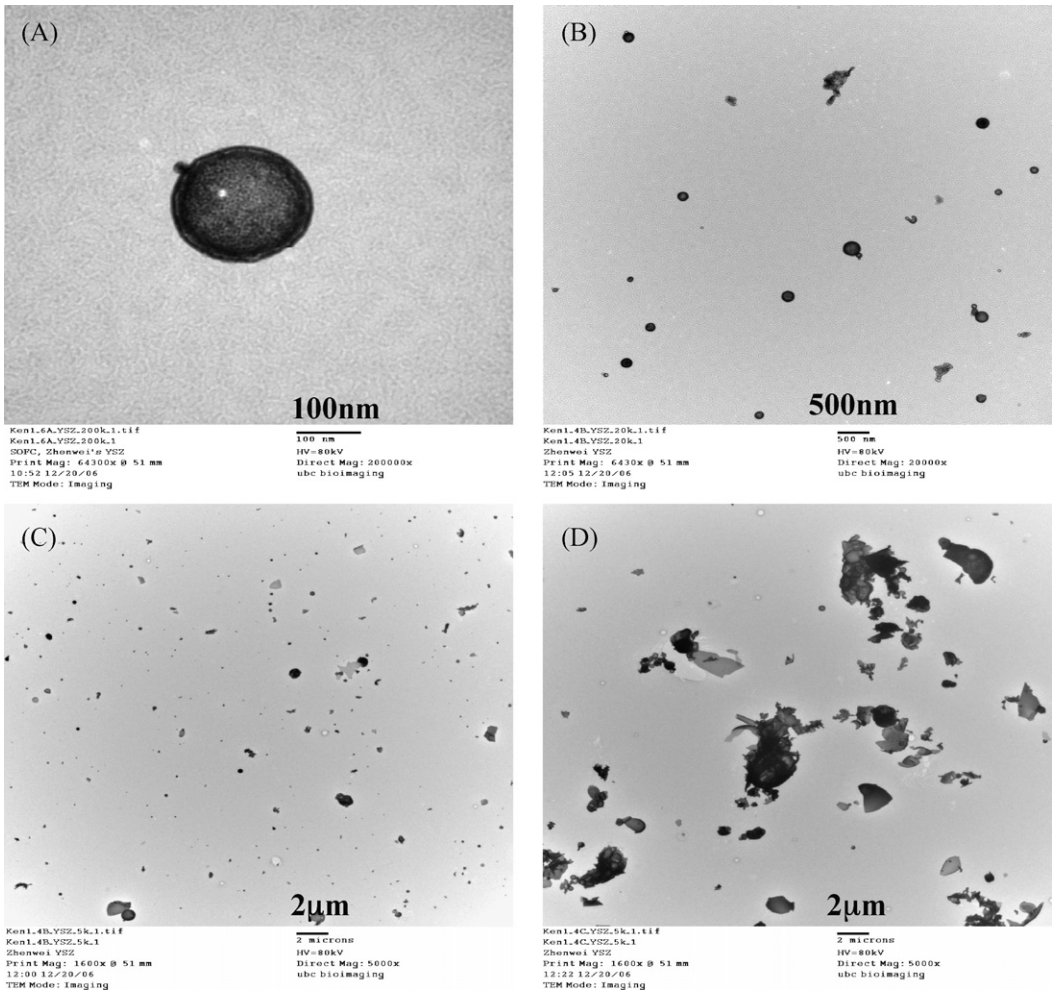

Fig. 4. (A–D) TEM photos of the plasma sprayed powder.

Table 1
Comparison of PSA and BET results

Sample	Conditions	PSA (μm)	BET ($m^2\,g^{-1}$)	D_{BET} (nm)
061108-2	No additive	1.769	12.2	83
061115-2F	Organic additive	2.145	20.0	50
061115-2F	Organic additive calcined at 600 °C for 2 h	1.937	27.0	37

in more concentrated TEM sample, as shown in Fig. 4D. Fig. 5 gives the plot of particle size distribution for the sprayed powder. PSA result shows the powder has a mean particle size of about 1.3 μm with broad particle size distribution (100 nm to 10 μm). Large particles (>5 μm) are also detectable, although they are only a small proportion of the total particles. According to the results of TEM and PSA, weak agglomeration of smaller fine grains exists in the sprayed powders. Besides the high surface energy of the fine powders, the surface charge from the plasma environment could be another possible reason, which significantly modifies the surface properties of the sprayed powder.

3.4. Organic additive

Organic additive in a stock solution can produce large amount of gases under plasma temperature with the assistance of air, and thus makes the sprayed powder looser. Moreover, the gas can adsorb plasma energy and in turn reduce energy density. In this way, formation of powder with fine grain size is expected. Table 1 shows the effects of the organic additive on powder characters. With the introduction of an organic additive, the BET area can be improved from 12.2 to 20.0 $m^2\,g^{-1}$. Consequently, the equivalent particle size decreases from 83 to 50 nm. However, a large amount of thermal gravimetric loss can be observed, as shown in Fig. 6. Freshly sprayed powder gives a total weight loss of about 19 wt.% up to 800 °C. The weight decrease before 150 °C should be attributed to the absorbed water, which is mainly introduced in the powder collection step. Other weight losses originate from the incomplete decomposition of nitrates and organic additive. The incomplete decomposition comes from the weakness of the applied plasma power and the length control of the plasma plume. Using a higher plasma power and a longer plasma plume can avoid this incomplete decomposition. In this case, however, lower specific surface area and larger grain size would be resulted. With the powders post-calcined at 600 °C for 2 h, the nitrates and organic leftover are fully burned off and the specific surface area increases significantly from 20.0 to 27.0 $m^2\,g^{-1}$, as shown in Table 1. D_{BET} also shows a slight decrease from 50 to 37 nm after post-treatment.

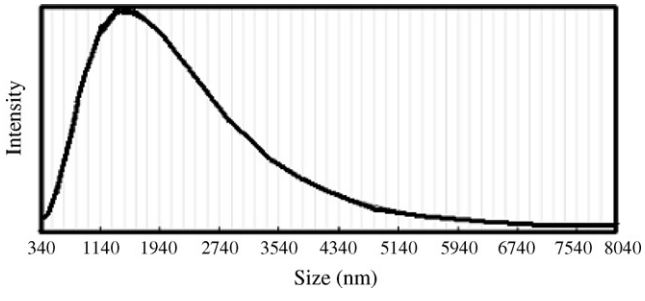

Fig. 5. Particle size distribution of the plasma sprayed powder tested in water solution with DARVIN C as dispersant.

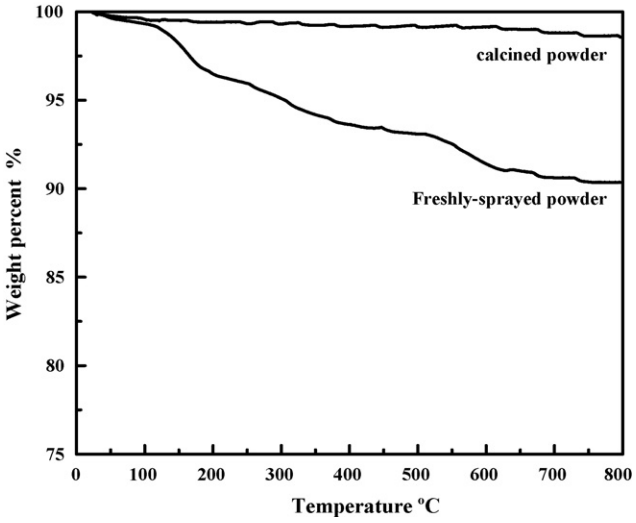

Fig. 6. TG results of the freshly sprayed powder and the calcined one.

4. Conclusions

A simple, cost-effective and easily scaled process for the nano-YSZ powder production method through plasma spray routine has been developed in Northwest Mettech Corp. and significant technical developments have been achieved during the past 2 years. Pure YSZ powders with cubic phase can be obtained without obvious impurities species. BET specific surface area of sprayed powder reaches as high as 27 $m^2\,g^{-1}$, indicating an equivalent particle size of 37 nm. Mean particle size by TEM observation is about 100–200 nm while the powder shows weak agglomeration. Considering the significant time- and cost-saving, plasma spray process shows promising potential for the mass production of ultra-fine oxide powders for solid oxide fuel cells.

Acknowledgements

The authors gratefully acknowledge financial support from Northwest Mettech Corp. based on the project of "Production of Nanopowder for Solid Oxide Fuel Cells Using Axial Injection Plasma Spray".

References

[1] Z. Wang, M. Cheng, Y. Dong, M. Zhang, H. Zhang, Solid State Ionics 176 (2005) 2555–2561.
[2] Z. Wang, M. Cheng, Y. Dong, M. Zhang, H. Zhang, J. Power Sources 156 (2006) 306–310.
[3] Z. Wang, M. Cheng, Z. Bi, Y. Dong, H. Zhang, J. Zhang, Z. Feng, C. Li, Mater. Lett. 59 (2005) 2579–2582.
[4] L. Combemale, G. Caboche, D. Stuerga, D. Chaumont, Mater. Res. Bull. 40 (2005) 529–536.
[5] X. Xin, Z. Lü, Z. Ding, X. Huang, Z. Liu, X. Sha, Y. Zhang, W. Su, J. Alloys Compd. 425 (2006) 69–75.
[6] C. Viazzi, A. Deboni, J.Z. Ferreira, J.P. Bonino, F. Ansart, Solid State Sci. 8 (2006) 1023–1028.
[7] C. Laberty-Robert, F. Ansart, S. Castillo, G. Richard, S. Castillo, G. Richard, Solid State Sci. 4 (2002) 1053–1059.
[8] Y. Jiang, S.V. Bhide, A.V. Virkar, J. Solid State Chem. 157 (2001) 149–159.
[9] N.H. Kwon, G.H. Kim, H.S. Song, H.L. Lee, Mater. Sci. Eng. A299 (2001) 185–194.
[10] E. Djurado, E. Meunier, J. Solid State Chem. 141 (1998) 191–198.
[11] M. Gaudon, E. Djurado, N.H. Menzler, Ceram. Int. 30 (2004) 2295–2303.
[12] N.H. Menzler, D. Lavergnat, F. Tietz, E. Sominski, E. Djurado, W. Ficher, G. Pang, A. Gedanken, H.P. Buchkremer, Ceram. Int. 29 (2003) 619–628.
[13] G. Dell'Agli, G. Mascolo, J. Eur. Ceram. Soc. 20 (2000) 139–145.
[14] Y.B. Khollam, A.S. Deshpande, A.J. Patil, H.S. Potdar, S.B. Deshpande, S.K. Date, Mater. Chem. Phys. 71 (2001) 235–241.
[15] Q. Zhu, B. Fan, Solid State Ionics 176 (2005) 889–894.
[16] R.R. Piticescu, C. Monty, D. Taloi, A. Motoc, S. Axinte, J. Eur. Ceram. Soc. 21 (2001) 2057–2060.
[17] Z. Hua, X.M. Wang, P. Xiao, J. Shi, J. Eur. Ceram. Soc. 26 (2006) 2257–2264.
[18] C. Laberty-Robert, F. Ansart, D. Deloget, M. Gaudon, A. Rousset, Mater. Res. Bull. 36 (2001) 2083–2101.
[19] K. Prabhakaran, A. Melkeri, N.M. Gokhale, S.C. Sharma, Ceram. Int., available online September 12, 2006.
[20] K.A. Singh, L.C. Pathak, S.K. Roy, Ceram. Int., available online September 25, 2006.
[21] J.C. Ray, R.K. Pati, P. Pramanik, J. Eur. Ceram. Soc. 20 (2000) 1289–1295.
[22] A. Tarancón, G. Dezanneau, J. Arbiol, F. Peiró, J.R. Morante, J. Power Sources 118 (2003) 256–264.
[23] J. Yang, J. Lian, Q. Dong, Q. Guan, J. Chen, Z. Guo, Mater. Lett. 57 (2003) 2792–2797.
[24] M.L. Laue, H.G. Jiang, R.J. Perez, J. Juarez-Islas, E.J. Lavernia, Nanostruct. Mater. 7 (1996) 847–856.
[25] T.D. Xiao, K.E. Gonsalves, P.R. Strutt, P.G. Klemens, J. Mater. Sci. 28 (1993) 1334–1340.
[26] G. Schiller, T. Franco, R. Henne, M. Lang, R. Ruckdaschel, Electrochem. Soc. Proc. 16 (2001) 885–894.
[27] D. Stöver, D. Hathiramani, R. Vaßen, R.J. Damani, Surf. Coat. Technol. 201 (2006) 2002–2005.
[28] G. DiGiuseppe, Electrochem. Soc. Proc. 07 (2005) 322–333.
[29] R. Hui, Z. Wang, O. Kesler, L. Rose, J. Jankovic, S. Yick, R. Maric, D. Ghosh, J. Power Sources, in press.
[30] S. Hui, X. Ma, H. Zhang, H. Chen, J. Roth, J. Broadhead, A. Decarmine, M. Wang, T. Xiao, International Patent, WO 2003, 03/075383 A2.
[31] S. Hui, H. Zhang, J. Dai, X. Ma, T.D. Xiao, D.E. Reisner, 8th International Symposium on Solid Oxide Fuel Cells (SOFC-VIII), Paris, France, April 27–May 2, 2003.